LDEF MATERIALS DATA ANALYSIS: REPRESENTATIVE EXAMPLES

Gary Pippin and Russ Crutcher
Boeing Defense & Space Group
Seattle, WA 98124-2499
Phone:206/773-2846, Fax:206/773-4946

Part of the philosophy which guided the examination of hardware from the Long Duration Exposure Facility (LDEF) was that materials present at multiple locations should have fairly high priority for investigation. Properties of such materials were characterized as a function of exposure conditions to obtain as much data as possible for predicting performance lifetimes. This paper summarizes results from examination of several materials from interior locations of LDEF, selected measurements on silverized teflon blanket specimens, and detailed measurements on the copper grounding strap from tray D11.

Visual observations of interior locations of LDEF made during deintegration at KSC showed apparent changes in particular specimens. This inspection lead to testing of selected nylon clamps, fiberglass shims and heat shrink tubing from wire harness clamps, and visually discolored silver coated hex nuts.

Ten nylon wire support clamps were taken from a sampling of the same locations as the heat shrink tubing samples we tested, examined and compared with the condition of a virgin nylon 6/6 specimen. In general only slight changes in the properties of the space exposed nylon hardware were noted. All nylon clamps performed their function; although cracking was observed in five of the ten space exposed specimens we examined.

There was no change in the shore D hardness or the melting points of the space hardware relative to the ground control specimens. Specific heats of the space flown hardware increased by 10-20% relative to the nylon 6/6 control specimen. However, there is considerable variation in the value of specific heat of nylons so the difference may not be real.

All the space flown specimens show increased degradation products during pyrolysis gas chromatography. Infrared measurements showed peaks associated with bond rupture at amide linkages for all flight specimens, one of which also showed evidence of slight surface oxidation.

The changes observed are all indicative of some UV exposure but this is hard to quantify. These specimens likely received solar exposure for short periods of time through small gaps at the corners of the experiment trays. The slight oxidation on one individual specimen suggests that specimen was directly aligned with an opening near the leading edge. Thermal vacuum cycling also likely contributed to the crack development and embrittlement as the materials outgassed over time.

Initial inspection showed substantial discoloration on the surface of the silver coated hex nuts which held titanium clamps on the interior of the space and earth ends. Surface examination showed that this was due to a molecular contamination layer and that the silver surface was not oxidized to any significant degree. A few of the hex nuts were cross sectioned and the good condition of the hardware was confirmed.

Visual inspection of aluminum wire harness clamps, partially covered by heat shrink tubing with fiberglass shims inside, showed a distinctly different pattern along the longeron between rows 3 and 4 relative to all other locations. Around each wire harness clamp assembly on this longeron was a discolored area which appeared to be the result of outgassing from components of the wire harness clamp assembly. This pattern was not evident on any of the other longerons. Outgassing measurements from selected pieces of heat shrink tubing and shims lead to the following conclusions. Flight specimens of heat shrink tubing show total mass loss (TML) from outgassing measurements about 65-75% of the TML measured for

ground control specimens. Table 1 shows average TML and collectable volatile condensible materials (CVCM) for heat shrink tubing specimens from selected locations. These specimens were taken from a portion of the tubing directly exposed to the interior of LDEF. An additional set of measurements were made on specimens from a portion of each tubing piece facing the longeron. Each number in the table is an average of four individual measurements.

There are two populations among the space exposed specimens, leading and trailing edge locations form one group and all other locations form the second group with the lowest TML values. The CVCM values are generally lower for space exposed specimens relative to the ground specimens, and the non leading or trailing edge specimens have the lowest CVCMs. The reason for these differences is not well understood. However, the leading and trailing edges did see the most solar UV and the thermal cycling patterns varied from location to location, so indirect heating effects could have caused the differences. Another possibility is that differing amounts of intermittent direct solar UV radiation reached the clamps through gaps at the tray corners. Figures 1 and 2 show the TML and CVCM data plotted as a function of the angle from the nearest of either the leading or trailing edge.

Outgassing of a small sampling of fiberglass composite shims was measured. TML for flight specimens was 85-95% of the ground control value, with no apparent differentiation due to location.

Modeling efforts have now provided a reasonable estimate of solar fluence to each major surface of LDEF. Earlier measurements characterizing the effects of solar UV on fluorinated ethylene propylene (FEP) have been revisited. X-ray photoelectron spectroscopy (XPS) measurements were carried out on the surface of FEP films from many locations on LDEF. The carbon 1s peak heights for carbon atoms in different locations in the FEP polymer change with exposure to solar UV. This change is induced by the breaking of carbon-carbon bonds, subsequent crosslinking between polymer chains or decomposition and loss of volatile fragments, leading to a polymer of different structure than the initial FEP. While exposure to AO leads to oxidation, volatilization and recession of the UV altered material, trailing edge specimens retain the altered layer of material and allows characterization of the solar UV effects.

It is observed that increased UV exposure increases the fraction of -CF and CF_3 functional groups at the expense of the CF_2 groups along the chain. The structural changes associated with this are increased crosslinking and embrittlement of the near surface material.

Detailed measurements have been carried out on two trailing edge blankets, D01 and C05. Measurements at selected locations in protected areas, exposed areas and in the curved region of each blanket show variation in the surface properties. The UV exposure for each location in the curved region has yet to be determined.

Specimens from the leading edge show ratios essentially independent of the UV exposure. This is consistent with the removal of UV damaged material by atomic oxygen, leaving virgin FEP on the surface, particularly since the majority of the oxygen exposure occurred in the last six months of the mission, after most of the UV damage had occurred. Figures 3-4 summarize these results graphically. Figure 5 shows how the ratio varies around LDEF, with row 6 clearly a transition region from atomic oxygen dominated processes to solar UV dominated processes.

The curved transition region of each blanket between the exposed face and shielded edge provides the basis for extensive recession vs angle data. Several methods were used to determine the angle from ram of the surface as a function of distance from the shielded edge of the blanket. SEM images were obtained and the angle from ram estimated from the direction of the textured peaks. This provided angles to within about 5 degrees and allowed identification of the location on the blanket surface facing the ram direction to within 2mm. We also examined photographs of blanket edges, taken with the blankets still mounted on the flight experiments, to attempt to define the radius of curvature. A spare blanket was remounted in a tray at ESTEC in an attempt to determine the flight configuration geometry and measure the curvature of the transition region from exposed to shielded areas. To calculate recession of FEP using our AO exposure

model we assumed the radius of curvature was constant. This reproduced the experimental values to within the measurement uncertainty.

An angle bracket from the McDonnell-Douglas heat pipe experiment on tray F9 provided an exposed area of FEP mounted with a well defined orientation with respect to ram. The FEP/Ag blanket was adhesively bonded to an aluminum bracket, shown in cross section in Figure 6. The rigid aluminum established a continuous range of well defined angles from about 8°to 90° from ram. An area of the angle bracket was mounted in a potting compound, cut and polished in cross section, 100X photomicrographs were taken of the cross section all along the length of the bracket, and the thickness of the FEP layer measured directly from the photomicrograph images. The thickness of the FEP along the bracket measured in this manner agrees with results obtained using our atomic oxygen exposure model, which includes the contribution from directly impacted and scattered atomic oxygen, to within the measurement uncertainty. To determine recession rates we used a reaction efficiency of 0.34×10^{-24} cm^3/atom, independent of angle of incidence.

Figure 7 shows the thickness vs angle data. The diamond shaped individual data points are from the raised part and the convex curved portion of the bracket. The triangle shaped individual data points are from the lower part and the concave curved portion of the bracket. The decreased thickness at or near the concave region, relative to the thickness of the raised portion is attributed to enhanced atomic oxygen exposure due to indirect scattering. Figure 8 shows the thickness vs location from photomicrograph cross-sections of two specimens from the edge of the blanket on tray D11. Curved and flat refers to the way the specimens were mounted in the potting compound for cross sectioning. The two specimens gave virtually identical results.

The exposed surfaces of the copper grounding straps had a rather complex geometry. Two areas on each clamp had well defined orientations; the portion on top of the clamps holding the experiment trays and the portion along each tray lip. Each exposed clamp and tray lip were at a 15° angle from one another. Measurements of solar absorbance and thermal emittance taken on surfaces from the areas with constant, well defined exposures, are shown as functions of atomic oxygen fluence and solar exposure in figures 9 and 10, respectively. Values for ground control specimens are plotted as zero exposure. No change in emittance is observed due to either leading or trailing conditions. The absorptance values for trailing edge specimens show no change over the exposure range 7000 to 11,000 equivalent sun hours, but these values are all substantially higher than the value for the ground control. This means that net UV induced changes occurred during the first half of the mission. The changes in absorbance on the leading edge exposed copper surfaces is a strong function of atomic oxygen fluence. Preliminary examination showed the darkened surface layer to be extremely thin, but the actual thickness has not been quantified.

The copper straps were made by bonding together two strips of 3M (X-1181) adhesive backed tape. The tape is manufactured into a roll and the release paper which protected the adhesive prior to use was coated with silicone. This caused a layer of silicone to be left on the copper as the tape was removed from the roll. Figure 11 shows a cross sectional view of the D11 copper strap flight configuration. The actual strap continued underneath the FEP where it was completely shielded from the UV and AO. XPS measurements were taken at many locations along the strap.

The surface elemental composition of the strap portion shielded by the aluminum shim was essentially identical to the surface elemental composition of a ground control strap. The relative atomic oxygen flux was determined along the D11 strap by using our atomic oxygen exposure model. The curve plotted in Figure 12 shows the flux from where the strap appears from under the FEP/Ag blanket (~22mm) to past the point where it goes beneath the shim. At distances greater than ~105mm the exposed surface is the aluminum shim and bolt rather than the copper. The copper surface was directly exposed to ram oxygen around 40mm from the physical end of the copper strap. XPS shows wide variation in copper, oxygen, carbon and silicon mol fractions on the surface. Figures 13 and 14 show the copper and silicone data. Figure 15 shows a comparison of O/C XPS ratios vs. location on the strap in comparison with relative oxygen flux levels. The XPS analysis shows the mol % copper on the surface is very low for shielded regions under the FEP and shim, falls to zero for the strap portion between the tray wall and FEP, goes

through a small peak along the curved portion of the strap which passes through the ram direction, and then goes through a very large peak for the region of the strap along the edge of the clamp. This area saw enhanced atomic oxygen exposure due to scattered oxygen from the part of the clamp on the tray tip as well as direct impacts. This relatively "clean' area of the strap shows copper to be the major constituent on the surface. Examination of the silicon data shows a corresponding drop in intensity in this same area. The silicon elemental % shows two distinct patterns in the exposed portion of the strap. The area from the edge of the FEP along the tray wall and tray lip which was in view of the vent slots in the FEP blankets, showed increased mol % relative to the ground control sample and shielded part of the strap under the shim.

The exposed areas along the edge of the tray, and the tray clamp, which was directly exposed to atomic oxygen but not the potential contamination source from the blanket adhesive, showed decreased Si content relative to the ground control and covered areas of D11. Figure 15, showing a comparison of O/C surface elemental % ratio and oxygen flux as location on the strap, also supports the fact that outgassed siloxane material deposited on the lower exposed area of the clamps, increasing the % silicon and oxygen on these areas above that expected from the ground based contamination and the ambient atmosphere, respectively.

The nylon materials exhibited change consistent with some UV exposure. The heat shrink tubing and fiberglass shim flight specimens all show lower outgassing than corresponding ground control specimens. Contaminant deposits were observed on the trailing edge longeron and on the silver coated hex nuts. The heat shrink tubing space exposed specimens have two distinct populations, those from the leading and trailing edge longeron, and those from all other locations. Further differentiation would require measurements on a larger sample population.

The UV exposed FEP showed evidence of surface and near surface structural changes as measured by XPS. These changes, characteristic of bond breaking and molecular rearrangements by crosslinking between polymer chains, correspond to previous data showing embrittlement as measured by decreased elongation to failure, and lower tensile strength, with increasing UV.

Data was presented for recession due to exposure to atomic oxygen for locations with well-defined angles from ram. Related theoretical modeling work has shown that some indirect scattering by atomic oxygen is necessary to predict observed results.

The 3M X-1181 adhesive backed copper tape had a silicone coated release paper protecting the adhesive on the roll. This left a deposit of silicon on the bare copper. This deposit was enhanced in areas directly exposed to venting from the blanket interior and was reduced in areas with the greatest exposure to atomic oxygen. This implied that processes which compete with oxidation of silicones to silicates occurred and that these processes produced volatile silicon containing species which were removed. Areas with the largest fluence of oxygen had the most reduced levels of silicon, carbon, and oxygen.

The discolored, oxidized layer is extremely thin. Copper tape could be used as interconnects for solar cell arrays without the need for a protective coating. Examination of the copper straps also provided significant data on deposition of silicone based contamination.

Each of the materials discussed in this paper performed their engineering functions for the duration of the flight. Observed changes for materials on the interior were slight. UV induced changes in the FEP polymer film were considerable and did not appear to have reached equilibrium at 11000 hours. The recession data reported covers the most extensive range of angles from ram to date. This work was carried out at the direction of NASA Langley Research Center under contract NAS1-19247, as part of Boeing's responsibilities in support of the LDEF Materials Special Investigation Group.

Table 1 Outgassing Data for Heat Shrink Tubing Specimens

SPECIMEN LOCATION LONGERON BETWEEN ROWS, & BAY	TML(%)	CVCM(%)
3-4, A	0.113	0.050
3-4, B	0.130	0.069
3-4, C	0.122	0.060
8-9, B	0.137	0.051
8-9, B	0.123	0.053
5-6, B	0.100	0.049
D-8, D-E	0.103	0.050
9-10, B	0.132	0.061
9-10, F	0.113	0.047
10-11, C	0.115	0.057
Space End	0.111	0.044
2-3, E	0.136	0.061
12-1, E	0.114	0.045
Earth End	0.102	0.042
8-9, F	0.126	0.056
3-4, B	0.139	0.054
Ground Control	0.170	0.061

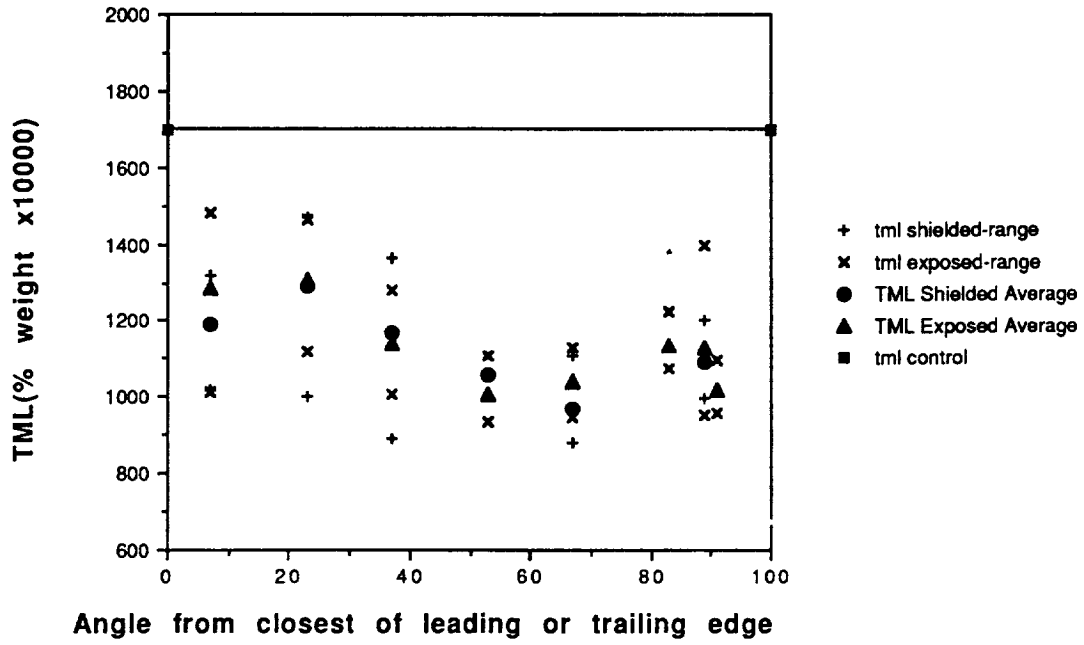

Figure 1 Total Mass Loss Outgassed from LDEF Heat Shrink Tubing Specimens

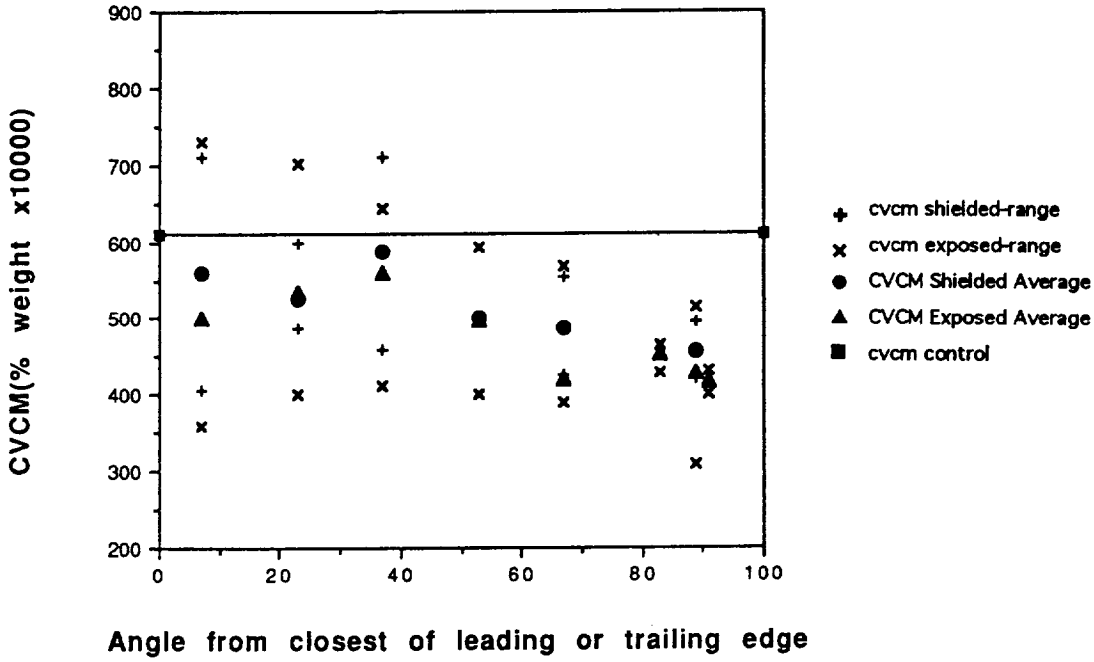

Figure 2 Collectable Volatile Condensible Materials Outgassed from LDEF Heat Shrink Tubing Specimens

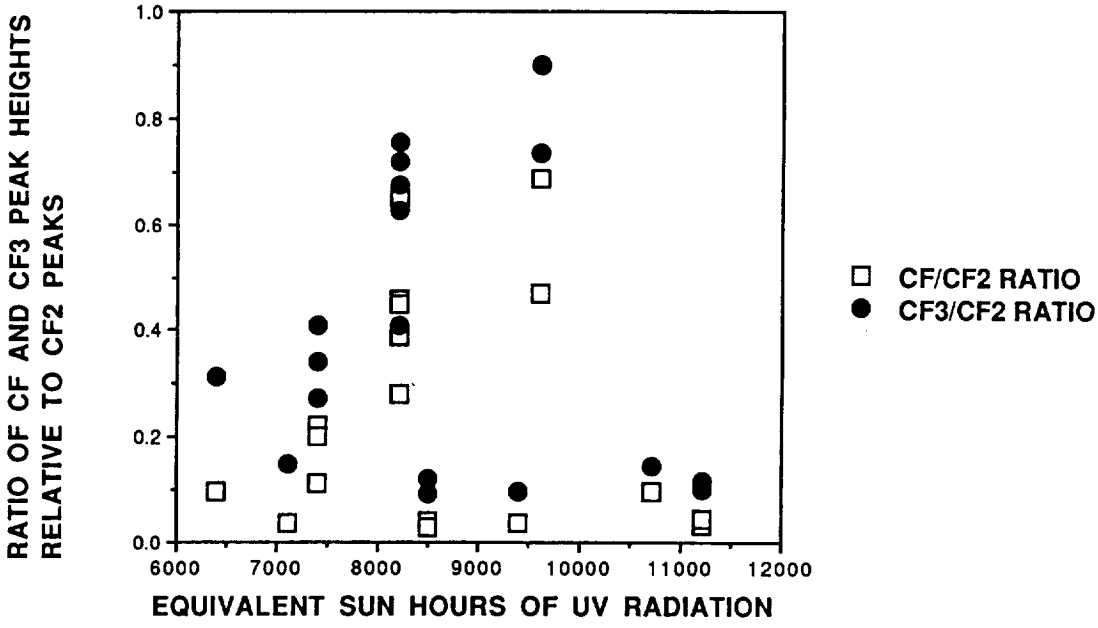

Figure 3 Structural Changes in FEP vs Solar Exposure for Silverized Teflon Blankets from LDEF

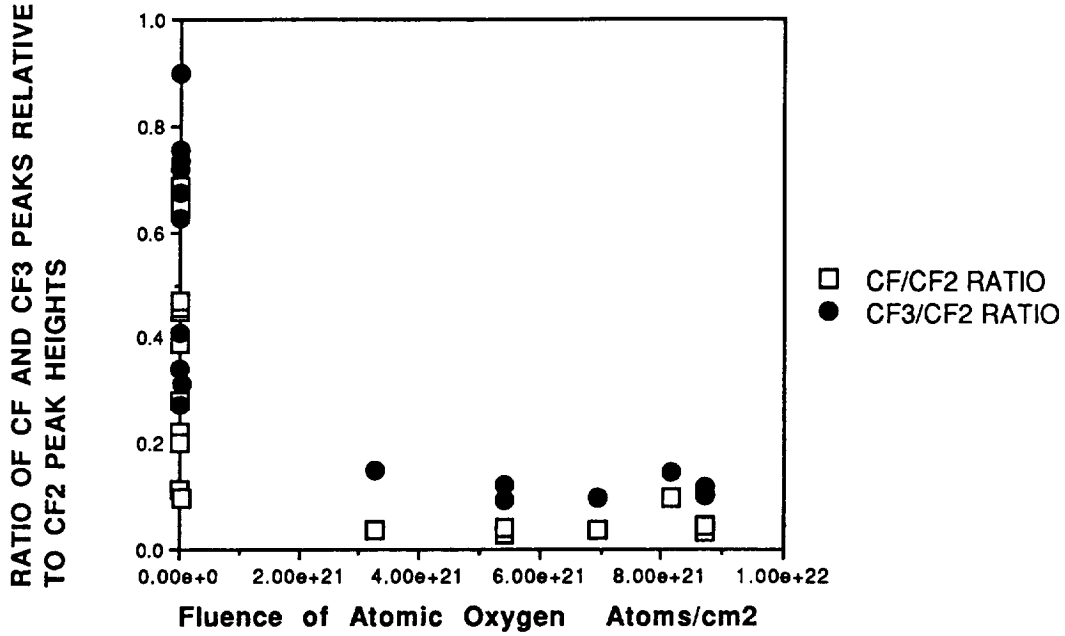

Figure 4 Structural Changes in FEP vs Atomic Oxygen Exposure for Silverized Teflon Blankets from LDEF

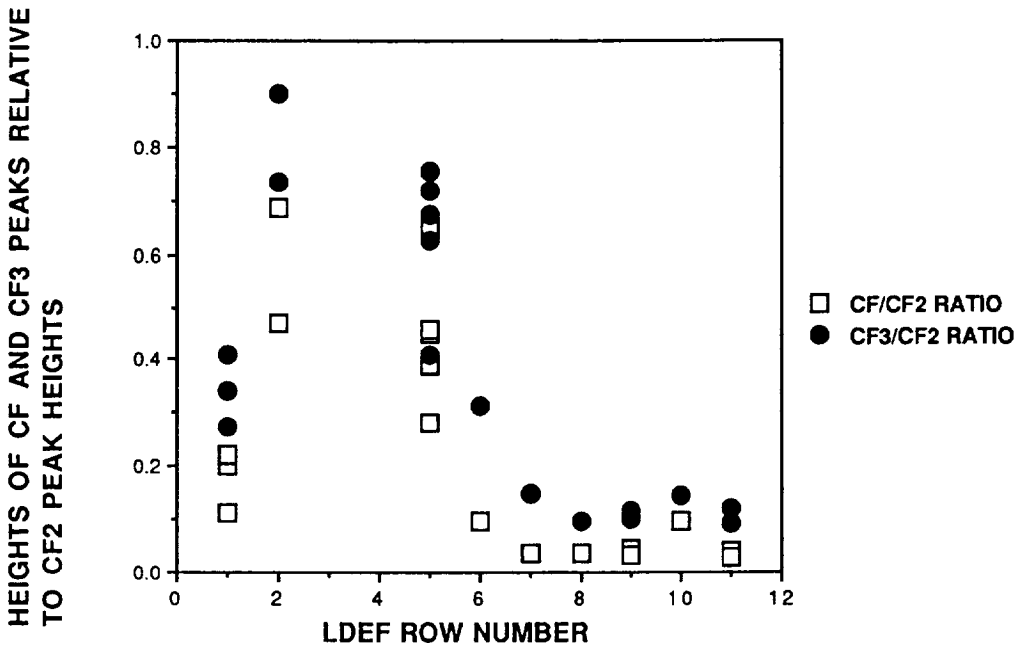

Figure 5 Evidence for Structural Changes in FEP Layer of Silverized Teflon vs Location on LDEF

Figure 6 Photograph of Piece of Angle Bracket and Mounted Specimen for Photomicrograph Cross-Section Thickness Determination

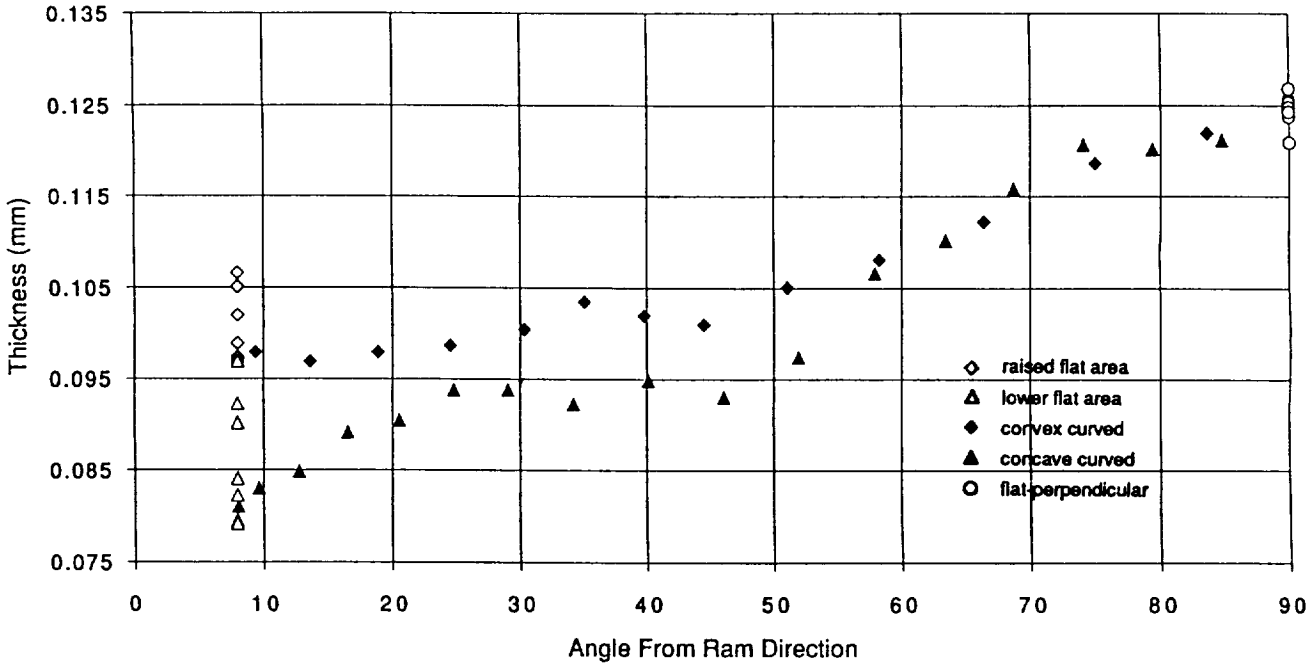

Figure 7 Erosion Rate Data for Exposed FEP from Silverized Teflon Thermal Control Blanket on Angle Bracket Mounted on LDEF Tray F9

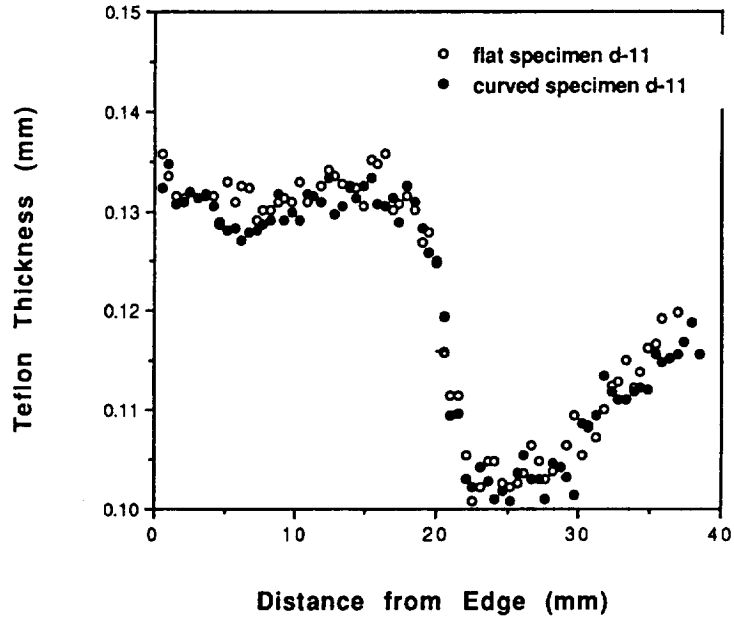

Figure 8 Atomic Oxygen Induced Erosion of FEP as a Function of Distance Along a Curved Portion(varying angle to ram) of Silverized Teflon Blanket from Tray D11

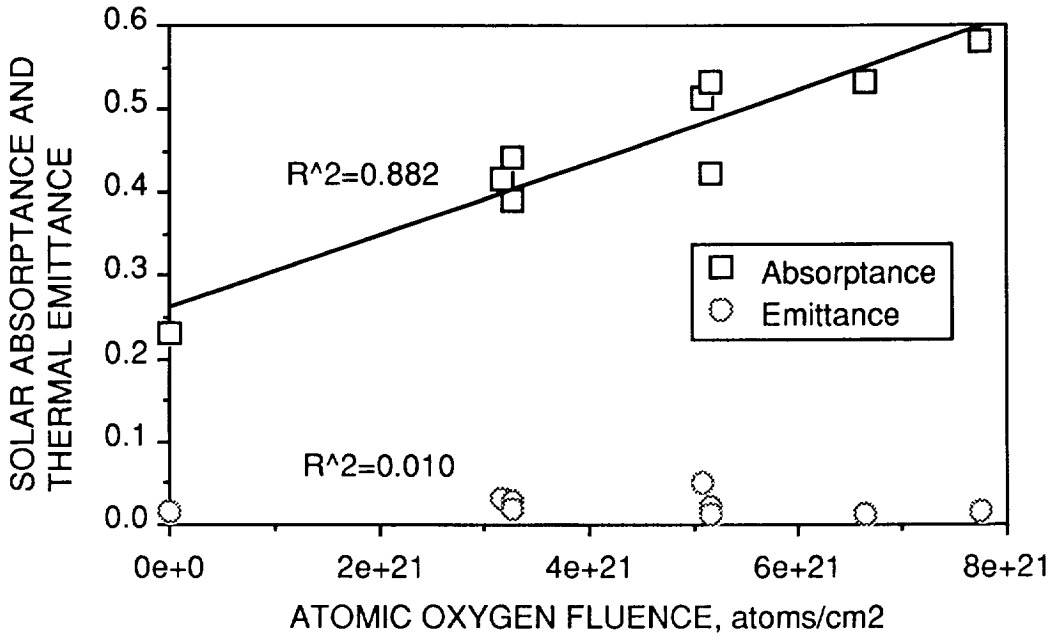

Figure 9 Optical Properties of Copper Grounding Straps from LDEF as a Function of Atomic Oxygen Exposure

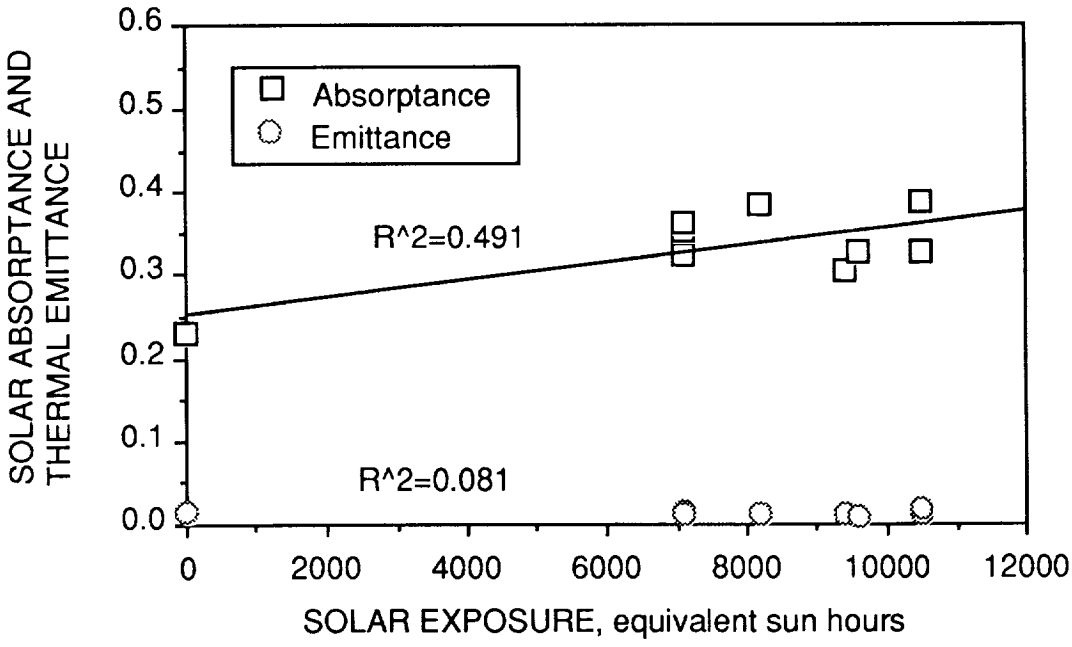

Figure 10 Optical Properties of Copper Grounding Straps from LDEF as a Function of Solar Exposure

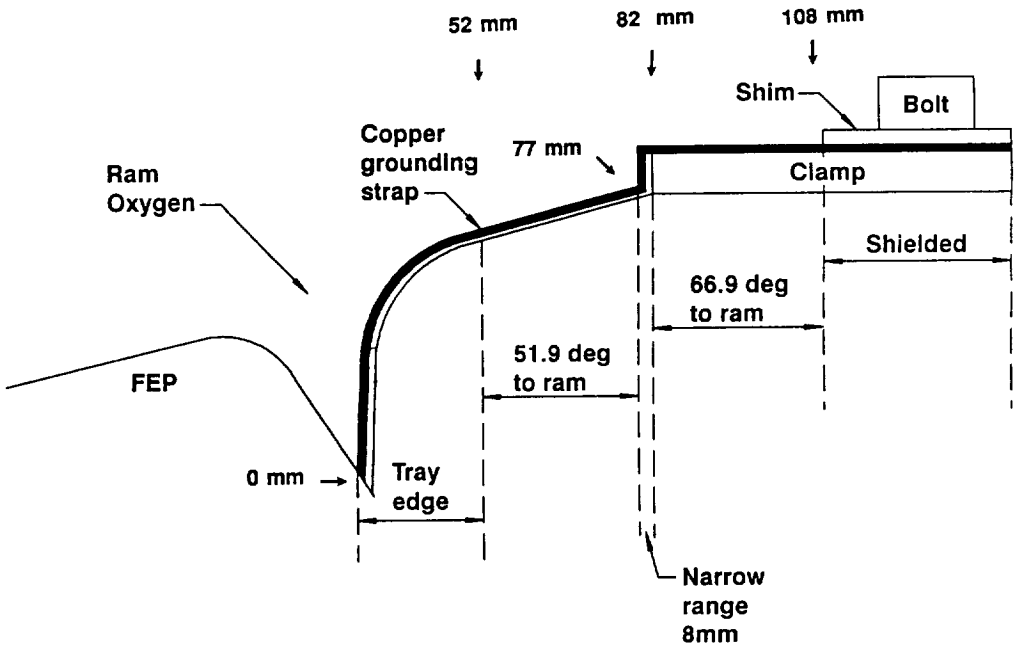

Figure 11 Cross Section View of Copper Grounding Strap, Tray D11, and Surrounding Structure

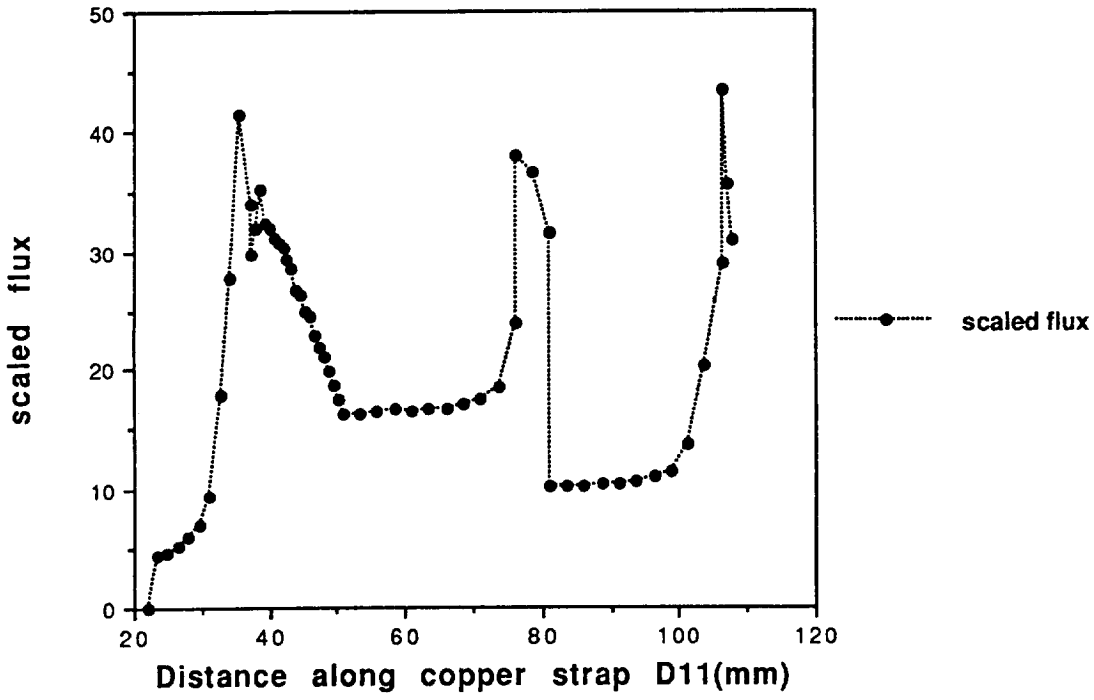

Figure 12 Relative Flux of Atomic Oxygen as a Function of Location on Copper Grounding Strap D11

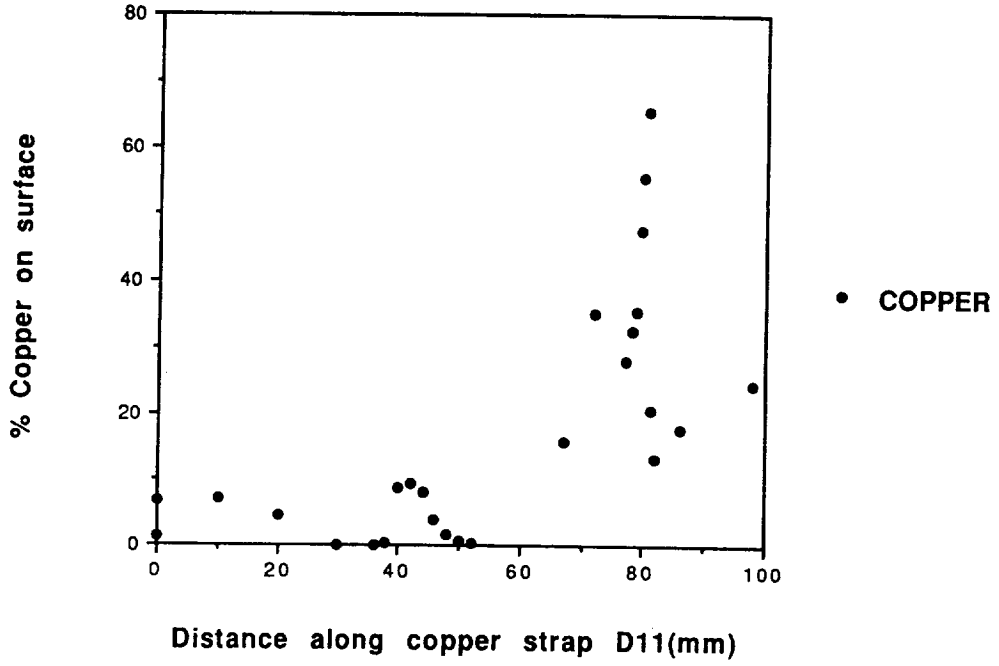

Figure 13 Copper Mol% as Measured by XPS, as a Function of Location on Surface of Copper Grounding Strap D11

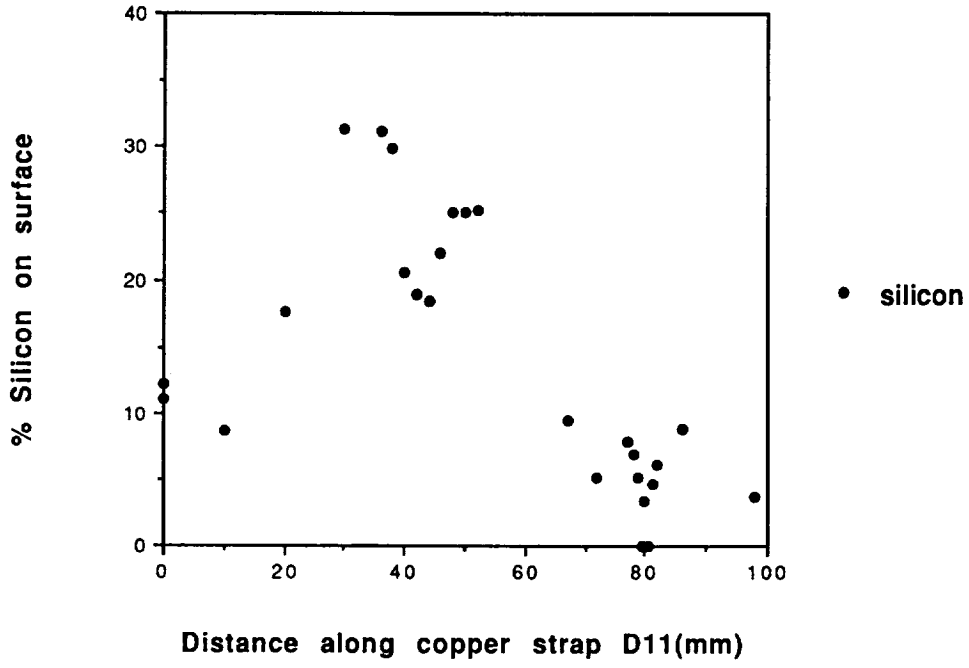

Figure 14 Silicon Mol % as Measured by XPS, as a Function of Location on Surface of Copper Grounding Strap D11

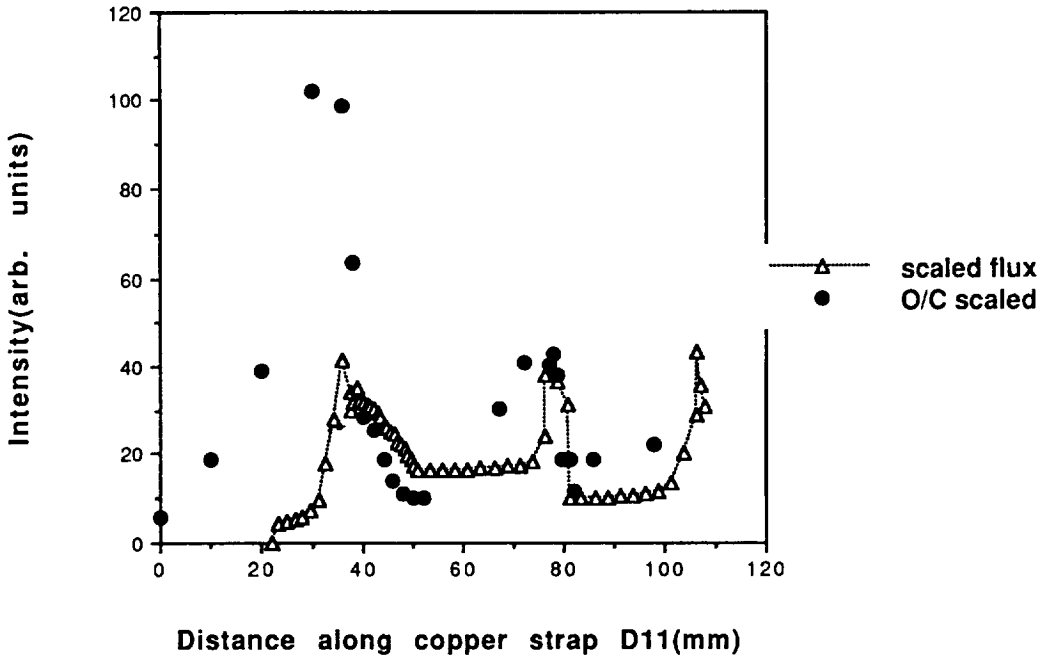

Figure 15 Comparison of Ratio of Oxygen to Carbon Mol % vs Location on Copper Strap with Atomic Oxygen Flux